Experimental Study of Parametric Autoresonance in Faraday Waves

Oded Ben-David, Michael Assaf, Jay Fineberg, and Baruch Meerson
The Racah Institute of Physics, The Hebrew University of Jerusalem, Jerusalem 91904, Israel
(Received 23 November 2005; published 19 April 2006)

The excitation of large amplitude nonlinear waves is achieved via parametric autoresonance of Faraday waves. We experimentally demonstrate that phase locking to low amplitude driving can generate persistent high-amplitude growth of nonlinear waves in a dissipative system. The experiments presented are in excellent agreement with theory.

DOI: 10.1103/PhysRevLett.96.154503 PACS numbers: 47.35.−i, 05.45.−a, 47.20.Ky

Introduction.—When a nonlinear oscillator is resonantly driven by small amplitude periodic forcing, the amplitude growth is arrested, even at zero dissipation, when nonlinearity comes into play. This is because a frequency mismatch develops between the (constant) driving frequency and the (amplitude dependent) oscillator frequency [1]. *Persistent* amplitude growth can be achieved, by autoresonance, when the system nonlinearly locks to an externally varied (''chirped'') driving frequency to retain resonant conditions. The precise form of the chirp is unimportant once its sign is correct, and the chirp rate is below a critical value. First predicted for harmonic forcing, autoresonance has found many applications [2]. The technique was extended to weakly dissipative oscillators [3] and to nonlinear waves and vortices in nondissipative systems [4]. The theory of *parametric* autoresonance (PAR) was recently developed, first for nonlinear oscillators [5] and later [6] for nonlinear Faraday waves: standing gravity waves on a free surface of a fluid which are excited parametrically by vertical vibrations. This theory [6] predicts that a downward chirp of the vibration frequency should cause persistent wave growth, which is only expected to terminate at large amplitudes, when an underlying *constant* frequency system (CFS), introduced below, ceases to exhibit a nontrivial stable fixed point.

Here we report the first experimental verification of PAR excitation of a nonlinear wave. Using Faraday waves we demonstrate that autoresonance is not hindered by moderate dissipation, and the results compare well with an extended version of the theory [6]. We show that the predicted (negative) frequency chirp indeed drives persistent wave growth, via the PAR mechanism, to amplitudes that surpass the theory's region of validity.

Theory.—The theory of PAR excitation of nonlinear Faraday waves [6] is based on an amplitude expansion that extends earlier constant-frequency treatments [7,8] to the chirped frequency case. Here we summarize the main predictions of Ref. [6] and extend the model by (i) introducing a more general form of driving acceleration, and (ii) taking a more complete account of dissipation.

Throughout this Letter we consider a rectangular fluid cell of length l, width w, and depth h in the x, y, and z directions, respectively. To avoid three-wave interactions [9] we assume that the surface tension corrections are small [10]. Furthermore, we assume a deep-water limit $h > l$ and a sufficiently small w so that the fluid motion is two dimensional, depending on x, z, and t. The vertical displacement of the vibrating cell is $\zeta(t) = \zeta_0(t)\cos\Phi(t)$, where $\Phi(t) = \int_0^t \omega(t')dt'$ is the driving phase, while the driving frequency $\omega(t)$ and amplitude $\zeta_0(t)$ vary slowly on the time scale of ω^{-1}. In the weakly nonlinear regime, the (time-dependent) scaled acceleration of the cell is $\varepsilon(t) = \omega^2(t)\zeta_0(t)/g \ll 1$, where g is the gravity acceleration. As a result, the wave steepness parameter $k\eta_{\max} \ll 1$, where $k = \pi/l$ is the wave number of the fundamental mode, and η is the wave amplitude. As the nonlinear frequency shift of standing gravity waves, in the deep-water limit, is negative [7], the PAR driving must use a negative frequency chirp: $d\omega/dt < 0$. The amplitude dynamics of the fundamental mode are governed, at leading nonlinear order, by the equation [6]

$$\ddot{\eta}_1 + 2\gamma\dot{\eta}_1 + \frac{k^2}{2}(5\dot{\eta}_1^2\eta_1 - 3\Omega^2\eta_1^3) + \Omega^2[1 + \varepsilon(t)\cos\Phi(t)]\eta_1 = 0, \quad (1)$$

where $\Omega = (kg)^{1/2}$ and $\gamma \ll \Omega$ are the linear wave frequency and *effective* linear damping rate, respectively (see Ref. [11] for a review of different contributions to γ). Higher-order modes are enslaved to η_1 and can be calculated once η_1 is found. For concreteness, we assume a linear chirp: $\omega(t) = \omega_0 - \mu t$, where $\mu > 0$ is constant, and $\omega_0 = 2\,\Omega$ is the resonant value of the driving frequency. We also assume $\varepsilon(t) = \varepsilon_0(1 + \beta t)$, where $\varepsilon_0 > 0$ and $\beta > 0$ are constant [12]. Now we make an ansatz $\eta_1(t) = A(t)\cos[\Omega t + \varphi(t)]$, where A and φ are the slowly varying amplitude and phase, and use the averaging method [1]. Rescaling time $\tau = (\varepsilon_0\Omega t)/4$, amplitude $B = kA\varepsilon_0^{-1/2}$, chirp rate $m = 8\mu/(\varepsilon_0\Omega)^2$, and damping rate $\Gamma = 4\gamma/(\varepsilon_0\Omega)$, and denoting $\phi(t) = \mu t^2/2 + \varphi(t)$ and $\tilde{\beta} = 4\beta/(\varepsilon_0\Omega)$, we obtain

$$\dot{B} = (1 + \tilde{\beta}\tau)B\sin(2\phi) - \Gamma B,$$
$$\dot{\phi} = (1 + \tilde{\beta}\tau)\cos(2\phi) - B^2 + m\tau, \quad (2)$$

where the dots stand for derivatives with respect to the slow time τ. The underlying CFS corresponds to $m = \tilde{\beta} = 0$. Let us start the frequency chirp from the steady state obtained for a constant-frequency driving (which is the stable fixed point of the underlying CFS). For small m and $\tilde{\beta}$, the PAR wave growth corresponds to the stable *quasifixed* point of Eq. (2). To leading order

$$B_*^2(\tau) = [(1 + \tilde{\beta}\tau)^2 - \Gamma^2]^{1/2} + m\tau,$$
$$\phi_*(\tau) = \frac{1}{2}\arcsin\left(\frac{\Gamma}{1 + \tilde{\beta}\tau}\right). \quad (3)$$

The PAR breaks down if the rescaled chirp rate m exceeds a critical value $m_{\rm cr} = \mathcal{O}(1)$ which depends on Γ [6] and $\tilde{\beta}$. In any case, the wave growth must terminate at large amplitudes, when higher-order corrections to Eqs. (1) and (2) cause the disappearance of the nontrivial stable fixed point in the underlying CFS [7,8].

Alternatively, we can start from a very small initial amplitude B_0 far from resonance and pass through the resonance. In the *linear locking stage*, we can drop the B^2 term in Eq. (2) and obtain [6]

$$B_*^2(\tau) \simeq B_0^2 \exp\left[\tau\sqrt{1 - (m\tau)^2} + \frac{\arcsin(m\tau)}{m} - 2\Gamma\tau\right],$$
$$\phi_*(\tau) \simeq \frac{\pi}{4} + \frac{1}{2}\arcsin(m\tau) - \frac{m}{4\sqrt{1 - (m\tau)^2}}, \quad (4)$$

where we have put $\tilde{\beta} = 0$. As long as $B_*(\tau) \ll 1$, Eq. (4) is valid on the time interval $-1 < m\tau < 1$ (but not too close to $m\tau = 1$ [6]). Remarkably, Eq. (4) corresponds to an *unstable* (saddle) quasifixed point [6], so the system eventually escapes from this point and either enters the *nonlinear* phase-locking regime, described by Eq. (3) with a shifted time, or loses phase locking. If or when $B_*(\tau)$ approaches unity, Eq. (4) becomes invalid. The amplitude $B_*(\tau)$, given by the first of Eq. (4), reaches a maximum at $\tau_m = \sqrt{1 - \Gamma^2}/m$. Its maximum value

$$B_*^{\max} \simeq B_0 \exp\left[\frac{1}{2m}(\arccos\Gamma - \Gamma\sqrt{1 - \Gamma^2})\right] \quad (5)$$

decreases with an increase of m. Therefore, at sufficiently large m Eqs. (4) and (5) remain valid over the whole interval $-1 < m\tau < 1$.

Experiment.—Our experiments were conducted in a transparent cell mounted on a Unholtz-Dickie model 5PM electromechanical shaker made to oscillate in the vertical (z) direction. At $\omega_0 = 54.7 \pm 0.16\ \mathrm{s}^{-1}$ we excite an almost pure gravity wave [10] with $k = 2\pi/8\ \mathrm{cm}^{-1}$, whose wavelength is twice the cell length of $l = 4$ cm. The cell of width $w = 2$ cm was filled to depth $h \simeq 6$ cm with hexamethyldisiloxane and sealed to prevent evaporation. Hexamethyldisiloxane is a Newtonian fluid whose kinematic viscosity, surface tension, and density are, respectively, 0.65 cSt, 15.6 dyn/cm, and 0.76 g/cc. The kinematic viscosity was stabilized to within $\pm 1.5\%$ by fixing the fluid temperature to $26.6 \pm 0.2\,^{\circ}\mathrm{C}$. We generated acceleration profiles of the form $a(t)\cos(\omega_0 t - \mu t^2/2)$ by computer. $a(t)$ was controlled to 1% and measured to 0.001 g resolution by an ADXL103 accelerometer.

Computer-triggered visualization of the wave profile was performed by uniform illumination of the fluid-air interface from behind. The interface's high curvature, due to its wetting of the side walls, refracted light away from a CCD camera mounted on the opposite side of the cell. This resulted in a sharp dark edge depicting the interface; see Fig. 1. A reference mark on the cell enabled measurement of its instantaneous vertical position. Edge detection produced a vector of the interface's location relative to the cell position as a function of time. The scaled amplitude of the fundamental, kA, measures the steepness of the wave profile. To enable direct comparison to theory, we needed to isolate the fundamental of the interface waveform. To this end, we measured the difference in wave elevation between two points, chosen to be symmetrical about the center of the cell on the x axis. This eliminates, by symmetry, all of the even harmonics of the interface elevation. Although the third harmonic is not filtered out, the resulting systematic error of A is only about 1% at $kA = 0.2$, and does not exceed 6% for $kA = 0.6$. We could therefore ignore the third harmonic while comparing our measurements with the theory in the weakly nonlinear regime. The statistical error in kA, as estimated from steady-state data, is $\sim 1\%$. The instantaneous phase mismatch ϕ between the driving and temporal response was extracted using complex demodulation [13] of two time series: the measured reference mark on the cell and the wave elevation.

In Fig. 2(a) we present the measured critical accelerations $a_c(\delta)$ for the Faraday instability of the flat surface as function of the scaled detuning $\delta \equiv (\omega_0 - \omega)/\omega_0$. The system undergoes a hysteretic transition [8] at another critical acceleration, $a_h(\delta)$: the lowest acceleration at which the nonlinear wave remains stable.

Figures 2(b) and 2(c) depict steady-state (CFS) measurements of kA and ϕ, respectively, as a function of δ for

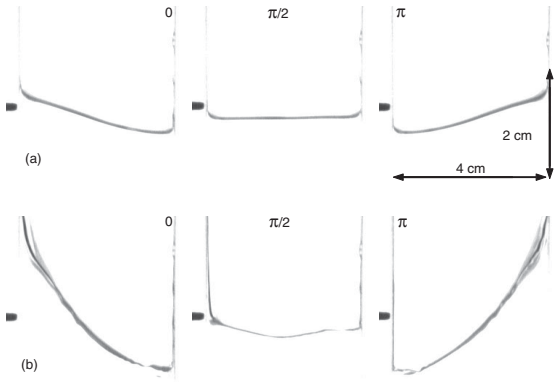

FIG. 1. Images at different phases of (a) an initial wave state at ω_0 and $a = 0.064$ g and (b) the same state after being autoresonantly driven at a chirp rate of $\mu = 0.2\ \mathrm{s}^{-2}$ to $\delta \equiv (\omega_0 - \omega)/\omega_0 = 0.08$ and $a = 0.113$ g.

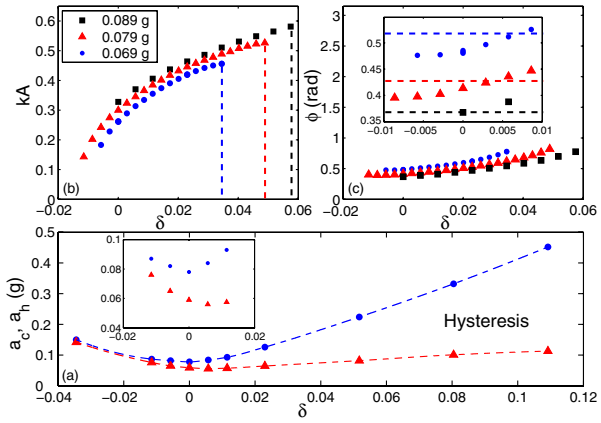

FIG. 2 (color online). (a) Measured δ dependence of a_c (circles) and the hysteretic region bounded by a_h (triangles). Dashed lines depict cubic interpolation. Inset: Close-up of the vicinity of $\delta = 0$. Steady-state measurements of kA (b) and ϕ (c) for different values of $a = \text{const}$ (legend) versus δ. Here $\Gamma \geq 0.65$. Dashed lines in (b) denote the maximum detuning attainable for each value of a. Inset of (c) is a close-up of the vicinity of $\delta = 0$; dashed lines depict the predicted values.

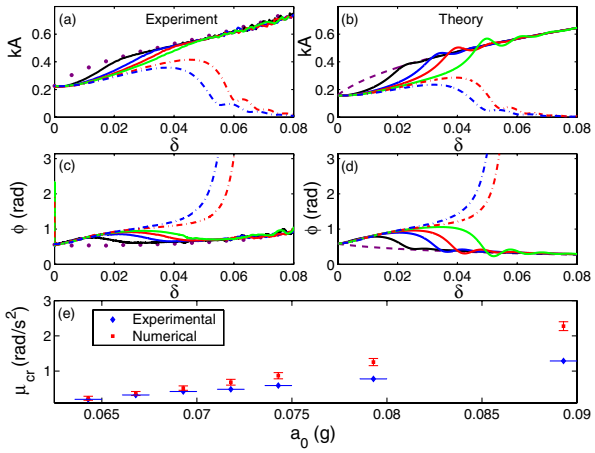

FIG. 3 (color online). Chirps in δ initiated from a fixed point. Measured (a) and computed from Eq. (2) (b) values of kA versus the detuning δ, starting from $\delta = 0$ and $a_0 = 0.064$ g. $\Gamma \simeq 0.9$. Chirp rates of $\mu = 0.09, 0.15, 0.18$, and $0.20\ \text{s}^{-2}$ (black to green/dark to light solid lines) converge to the fixed point (circles). kA for $\mu = 0.21$ and $0.25\ \text{s}^{-2}$ (red/light and blue/dark dash-dotted lines) diverge from the steady state and decay. The dashed line in (b) depicts the line of quasifixed points from Eq. (3). (c) and (d) are the measured and computed values of ϕ, respectively. (e) Experimental (diamonds) and computed from Eq. (2) (squares) values of μ_{cr} as a function of a_0.

$a = \text{const}$. Note that $a = a_h$ sets the maximum attainable detuning. Until $a = a_h$, kA increases rapidly with increasing δ (decreasing ω). Beyond this point, waves will rapidly decay.

The wave damping rate γ can be extracted from measurements of a_c, since $\Gamma = 1$ at the instability onset. With γ in hand, we can directly compare our measurements to theoretical predictions with no other free parameters. The measured phase difference for $\delta = 0$ agrees within 5% with the predicted value. The slow increase in ϕ with δ in Fig. 2(c) is due to higher-order nonlinearities.

Our first series of measurements used a linear chirp, $\delta = \mu t/\omega_0$, starting from a steady-state wave with a small but finite amplitude, at $\omega = \omega_0$ and $a = a_0 > a_h$. Importantly, our choice of the system parameters precluded the excitation of other linear modes during a negative chirp. As shown in Fig. 2(a), $a_h(\delta)$ is almost linear with δ for $0 \leq \delta < 0.12$. To maximize the frequency range of the excitation, we ramped a linearly in time, $a(\delta) = a_0 + \alpha\delta$, to make a nearly parallel ($\alpha = 0.609$ g) to $a_h(\delta)$.

An example of an autoresonant state achieved in a typical "ramping" experiment is shown in Fig. 1, where images at the initial and final values of δ are presented. Note the substantial increase in the wave amplitude. In Figs. 3(a)–3(d) we analyze the dynamics leading from Fig. 1(a) to Fig. 1(b) by comparing experimental measurements of kA and ϕ with theoretical predictions, obtained by integrating Eq. (2) numerically for several chirp rates for the same ramp and initial conditions [14]. For small values of μ, phase locking occurs where, as a function of δ, both kA and ϕ quickly converge to the values that they would attain in steady state for each instantaneous value of $a(t)$ and $\delta(t)$; see Eq. (3). At larger values of μ, however, *no* phase locking occurs. Here ϕ diverges rapidly away from the steady-state curves, and subsequently kA rapidly decays to zero.

As the theoretical curves were obtained with *no* free parameters, the agreement between experiment and theory is striking. Although the transients are slightly more long-lived in the theory, identical convergence or divergence of both the phase and amplitude of the waves to/from their steady-state values is observed for all of the values of μ used.

An important prediction of the theory is that above an a_0-dependent critical chirp rate, μ_{cr}, phase locking is not possible. For relatively small values of a_0, there is good quantitative agreement between the measured and predicted values of μ_{cr}; see Fig. 3(e). Furthermore, μ_{cr} still exists for larger accelerations. Even though μ_{cr} increases with a_0, as predicted, the predicted and observed values of μ_{cr} systematically diverge with increasing a_0. This divergence is not surprising, as for $a_0 > 0.07$ g the phase locking occurs for $kA > 0.4$, where we would expect the weakly nonlinear theory to become inaccurate. These results imply that PAR for $\mu < \mu_{\text{cr}}$ persists far beyond the region of validity of the weakly nonlinear approximation. Note that transient stages of ϕ in Fig. 3 trace an envelope, corresponding to the universal trajectory (a saddle point) obtained at $\mu = \mu_{\text{cr}}$ [6].

Our second series of measurements involves "passing through" the resonance at ω_0 before any waves are initially excited. We begin from a flat state at a negative detuning $\delta_{\text{init}} < 0$ (i.e., $\omega > \omega_0$), with $a_c(\delta = 0) < a < a_c(\delta_{\text{init}})$.

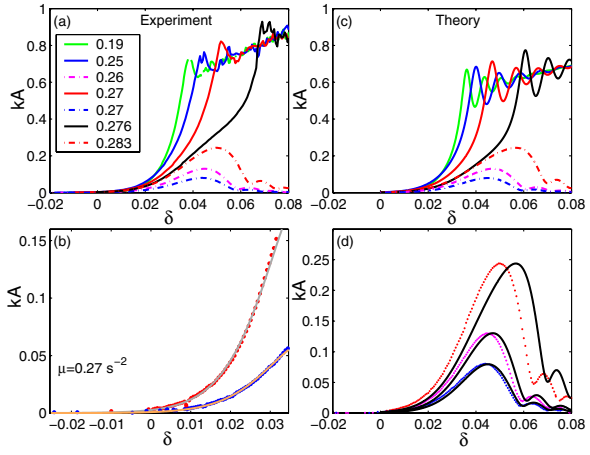

FIG. 4 (color online). Passing through resonance. (a) Measurements of kA for $a = 0.168$ g, $-0.046 < \delta < 0.08$. Solid (dash-dotted) lines depict phase locking (unlocking) for the values of μ (s^{-2}) presented in the legend. (b) Comparison of measured (dots) and computed from Eq. (4) (lines) values of kA in the initial stages of the two runs with $\mu = 0.27\ s^{-2}$. The different initial values of kA_0 [obtained by fitting Eq. (4)], resulting from low-level noise, determine the eventual behavior. (c) Computed values of kA, using Eq. (2), corresponding to the parameters of (a). (d) Comparison of computed (solid lines) and measured (dotted lines) values of kA for $kA < 0.3$.

We then apply a linear chirp $\delta = \mu t/\omega_0$ while keeping a fixed throughout the experiment. As δ is increased, we pass through a region of δ where $a > a_c(\delta)$.

The dynamics of passing through resonance are demonstrated in Fig. 4, where experimental measurements of kA as function of δ are shown for several chirp rates. As in Fig. 3, the distinction between phase locking at low values of μ and phase unlocked states at high values of μ is clear. A closer look at Fig. 4(a), however, reveals that the precise value of μ_{cr} is undetermined. Two different runs with the identical chirp rate of $\mu = 0.27\ s^{-2}$ have qualitatively different behavior: one decays, while the other phase locks into PAR. The difference in these two runs stems from the dependence of μ_{cr} on the wave's initial amplitude A_0. As the waves evolve from noise, we do not have experimental control over A_0. In Fig. 4(b) we present fits of the initial stages of both of the $\mu = 0.27\ s^{-2}$ trajectories shown in Fig. 4(a) to Eq. (4), where the sole fitting parameter is the value of A_0. In both the phase-locked ($kA_0 = 0.002\,69 \pm 0.000\,02$) and unlocked ($kA_0 = 0.0009 \pm 0.000\,04$) runs the experimental points are indistinguishable from the theoretical predictions. Thus, a difference of about 10 μm in A_0 ($\sim$0.1% of the final, phase-locked amplitude) is sufficient to determine the wave's long-time dynamics. Similarly, we obtained A_0 for all of the runs presented in Fig. 4(a) and, using these values, present the computed functions kA versus δ in Fig. 4(c), for the parameter values used in Fig. 4(a). As in Fig. 3, the theory, which uses no other free parameters, is a strikingly good description of the measurements, especially for values of $kA \leq 0.15$, where the weak nonlinearity condition $kA \ll 1$ is well satisfied. This is demonstrated in Fig. 4(d) where a close comparison of theory and experiment is performed for the three runs where phase locking failed. In the runs where $kA \leq 0.15$ throughout the entire experiment, theory and experiment are nearly indistinguishable. The agreement deteriorates when $kA > 0.2$, when the system is no longer in the weakly nonlinear regime.

In summary, one can control nonlinear Faraday waves by employing PAR. The PAR technique remains operational for moderate dissipation and well beyond the weak nonlinearity. It would be interesting to extend it to multimode regimes and to other examples of nonlinear waves.

This work was supported by the Israel Science Foundation (Grants No. 194/02 and No. 107/05). We thank G. Cohen for advice on all aspects of experiment.

[1] N. N. Bogoliubov and Y. A. Mitropolsky, *Asymptotic Methods in the Theory of Non-linear Oscillations* (Gordon and Breach, New York, 1961).
[2] J. Fajans and L. Friedland, Am. J. Phys. **69**, 1096 (2001).
[3] J. Fajans, E. Gilson, and L. Friedland, Phys. Plasmas **8**, 423 (2001).
[4] M. Deutsch, B. Meerson, and J. E. Golub, Phys. Fluids B **3**, 1773 (1991); I. Aranson, B. Meerson, and T. Tajima, Phys. Rev. A **45**, 7500 (1992); L. Friedland, Phys. Rev. Lett. **69**, 1749 (1992); Phys. Rev. E **59**, 4106 (1999).
[5] J. Fajans, E. Gilson, and L. Friedland, Phys. Rev. E **62**, 4131 (2000); E. Khain and B. Meerson, Phys. Rev. E **64**, 036619 (2001).
[6] M. Assaf and B. Meerson, Phys. Rev. E **72**, 016310 (2005).
[7] J. W. Miles, J. Fluid Mech. **75**, 419 (1976); **146**, 285 (1984); **248**, 671 (1993).
[8] S. Douady, J. Fluid Mech. **221**, 383 (1990); S. T. Milner, J. Fluid Mech. **225**, 81 (1991); M. Umeki, *ibid.* **227**, 161 (1991); A. D. D. Craik and J. G. M. Armitage, Fluid Dyn. Res. **15**, 129 (1995); S. P. Decent and A. D. D. Craik, J. Fluid Mech. **293**, 237 (1995).
[9] W. Zhang and J. Viñals, Phys. Rev. E **53**, R4283 (1996).
[10] In our experiments the surface tension correction to the linear wave frequency of the primary mode was less than 1% for the whole range of driving frequencies.
[11] B. Christiansen, P. Alstrom, and M. T. Levinsen, J. Fluid Mech. **291**, 323 (1995).
[12] The precise form of the $\varepsilon(t)$ dependence is of no importance, as long as $\varepsilon(t)$ stays above the hysteretic lower tongue and changes sufficiently slowly.
[13] V. Croquette and H. Williams, Physica (Amsterdam) **37D**, 300 (1989).
[14] The numerical results in Figs. 3(b) and 3(d) are within 15% from those obtained by directly integrating Eq. (1).